Green LSPR Sensors Based on Thin Bacterial Cellulose Waveguides for Disposable Biosensor Implementation

Nunzio Cennamo, Carlo Trigona, *Member, IEEE*, Salvatore Graziani, *Member, IEEE*, Luigi Zeni, Francesco Arcadio, Liu Xiaoyan, Giovanna Di Pasquale, and Antonino Pollicino

Abstract—**Nowadays there is an increasing request to realize green, eco-friendly, and biodegradable electronic devices for biosensor implementation. In this context, we have conceived and realized a green sensor based on localized surface plasmon resonance (LSPR) phenomenon in a thin-slab waveguide of bacterial cellulose (BC). These LSPR sensors can be obtained simply by gold sputtering on the slab BC waveguides. The performances have been studied investigating the presence of ionic liquids (ILs) inside and in absence of ILs with various thicknesses of the BC substrate. Depending of the thickness of the BC layer, the ILs effect on the LSPR can be constructive or destructive. In this work, we present a study of the sensor performances, in terms of bulk sensitivity and resolution by changing the aforementioned parameters. Analyses in terms of BC geometry are pursued in order to improve the interaction between the light and the LSPR phenomenon. The experimental setup used for this kind of extrinsic optical fiber LSPR sensor is based on two optical fibers used to connect a white light source and a spectrometer with the green LSPR sensor chip. Results evince the suitability of the proposed approach in order to realize sensors and biosensors with several intriguing properties and features. In fact, these LSPR platforms could be used to realize disposable biosensors, when a specific bioreceptor is covalently bonded to the gold.**

Index Terms—**Bacterial cellulose (BC), disposable green localized surface plasmon resonance (LSPR) sensors, eco-friendly sensors, LSPR, optical sensors.**

I. INTRODUCTION

THE realization of low-cost, disposable, and green sensors requires the development of new materials such as bioderived polymers. Several bioderived polymers can be considered. The most common one is cellulose, which represents

Nunzio Cennamo, Luigi Zeni, and Francesco Arcadio are with the Department of Engineering, University of Campania Luigi Vanvitelli, 81031 Aversa, Italy (e-mail: e-mail: nunzio.cennamo@unicampania.it).

Carlo Trigona and Salvatore Graziani are with the Department of Electrical, Electronics, and Computer Engineering (DIEEI), University of Catania, 95125 Catania, Italy.

Liu Xiaoyan is with the Department of Engineering, University of Campania Luigi Vanvitelli, 81031 Aversa, Italy, and also with the College of Electrical and Electronic Engineering, Changchun University of Technology, Changchun 130012, China.

Giovanna Di Pasquale is with the Dipartimento di Scienze Chimiche, University of Catania, 95125 Catania, Italy.

Antonino Pollicino is with the Department of Civil Engineering and Architecture, University of Catania, 95125 Catania, Italy.

a good candidate for the realization of green sensors, having intriguing features. Recently, another type of cellulose realized through bacteria and named bacterial cellulose (BC) has been proposed as a green base material for the realization of green transducers [1]–[4].

In particular, authors propose various sensing elements based on BC, impregnated with ionic liquids (ILs), and covered by polymeric electrodes (PEDOT:PSS) in order to measure displacement, mass, acceleration, and absorbed particles/optical channel [5]–[7]. This latter solution has already been investigated by some of the authors in order to realize an eco-friendly disposable plasmonic sensor based on BC and gold [8].

The plasmonic sensor is based on the advantage of surface plasmon resonance (SPR) phenomena and localized SPR (LSPR). Ground-breaking optical fiber biosensors are able to monitor different substances on-site and in real time, exploiting innovative plasmonic platforms and receptors. Thanks to their reduced size and low cost, they have been the object of research interest in many research fields, in conjunction with multiple receptor types [9]–[14]. Research has also been performed in order to optimize the efficiency and the performances of these sensors in terms of reliability, robustness, and miniaturization [15]–[20]. Both intrinsic and extrinsic optical fiber sensors can be simply realized. The sensing mechanism of an intrinsic optical fiber sensors is due to the interaction between the optical fiber and the analyzed medium [18]. Extrinsic optical fiber sensors exploit the fiber as a pure waveguide, which allows the light to enter the sensing area and to be connected [20]. Moreover, the optical fiber sensor configurations can be implemented in reflection mode, when the light source and the detector are placed on the same side of the fiber, or in transmission mode, when the light source and the detector are placed on opposite sides.

In this work, we will discuss about a green approach to realize a low-cost and disposable plasmonic sensor platform for biosensing, exploiting an extrinsic optical fiber configuration, used in transmission mode, based on an LSPR sensor chip realized by a BC slab waveguide covered by gold. In particular, we want to observe the effect of using ILs in thin BC waveguides. We have already investigated the role of ILs inside the BC waveguides, when the thickness of the BC waveguides is about 140 μm [8]. In this case (thick-slab

Fig. 1.   Picture of BC samples with (top) and without ILs (bottom).

Fig. 2.   FTIR ATR spectra BC, EMIM BF$_4$, and BC with EMIM BF$_4$ samples.

BC waveguides), we observed that the use of ILs decreases the sensor performances [8]. So in this work we reduced the thickness of the BC layer to exploit light scattering, induced by the ILs in the BC waveguide, to improve the plasmonic phenomenon. In fact, in a waveguide of reduced thickness, the scattered light can increase the amount of energy coupled to the LSPR instead of simply representing a net loss in the transmitted intensity [13], [14].

To validate the role of the ILs inside thin BC waveguides, in this work we have completed the experimental characterization of the configurations, with and without ILs inside thin BC waveguides while in [21], only preliminary results relative to one configuration of thin BC-ILs slab waveguide have been presented. After these new experimental results, a comprehensive comparative analysis about these LSPR-BC sensor configurations has been presented to choose the best configuration for biosensor implementation. In fact, when specific bioreceptors are used in contact with the gold nanostructures, exploiting self-assembled monolayers (SAMs) of receptors, the high performances of the chosen LSPR-BC platform can be used to monitor different substances, on-site and in real time, by disposable green LSPR biosensors. This aspect is important because disposable and low-cost biological and chemical sensors will be used in several application fields in the future (e.g., agriculture, food, environmental monitoring, security, and biomedical applications), with particular interest to green, biodegradable, and low-cost devices.

II. LSPR-BC Sensor and Experimental Setup

A. BC Samples: Production and Characterization

1-Ethyl-3-methylimidazolium tetrafluoroborate (EMIM-BF$_4$) was used as the ILs. The studied samples showed a large amount of absorbed ILs. In fact, gravimetric measurements showed an ILs absorption equal to 117% by weight. The treatment with ILs determined a morphology modification due to the disruption of the crystalline order in the BC, as testified by Fig. 1, where the significative transparency increase in the ILs treated film is evident.

Evidence of crystalline order modification can also be seen from FTIR ATR spectra, displayed in Fig. 2, where BC, EMIM BF$_4$, and BC with EMIM BF$_4$ are compared.

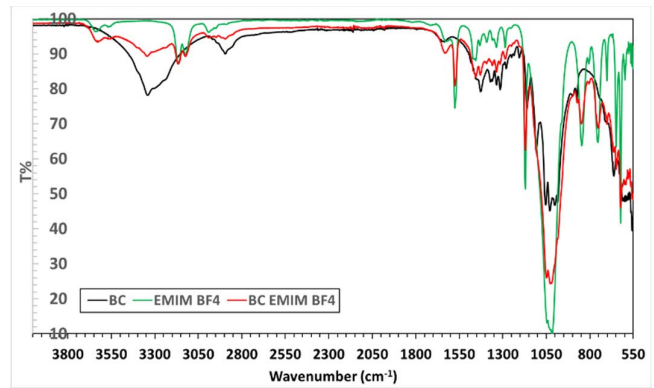These spectra were obtained using a Perkin–Elmer 100 Series Fourier Transform Infrared Spectrometer at r.t.

from 4000 to 550 cm^{-1}, with a resolution of 2 cm^{-1}. A universal ATR sampling accessory was used for the measurements, made directly on samples, without any preliminary treatment.

The main characteristic peaks of BC (dark curve in Fig. 2) are centered at about 3340.6 cm^{-1} (-OH stretching broaden by H bonds), 2893.9 cm^{-1} (-CH stretching), 1428.4 cm^{-1} (CH$_2$ scissoring), 1161.5 cm^{-1} (C-O-C antisymmetric stretching), and 1108.3 cm^{-1} (C-OH skeletal vibration). The ILs absorption (BC+EMIM BF$_4$ sample–red curve in Fig. 2) determines, beside the appearance of the peaks due to the IL (green curve in Fig. 2), the breaking of hydrogen bonds among cellulose molecules, and an increased content of free hydroxyl group, resulting in the reduction of the O–H stretching peak at 3344.3 cm^{-1} shifted to higher wavenumber because of the modification of the crystalline state of the BC. Such a shift is observed in other peaks too, such as the one centered at 2893.9 cm^{-1} in BC, centered at 2895.5 cm^{-1} in ILs treated BC, the 1428.4 cm^{-1} centered at 1429.2 cm^{-1} in ILs treated BC, and in the one centered at 1161.5 cm^{-1} in BC that shifts to 1170.4 in ILs treated BC.

The decrease in mass against temperature change of the studied samples were measured in static air by a Shimadzu model DTG-60 instrument. TGA curves have been recorded at a heating rate of 10 °C min^{-1}, under static air atmosphere, from 35 °C to 700 °C. The analyzed sample mass varied between 2 and 5 mg and the thermogravimetric curves and their first derivative curves are shown in Fig. 3. The thermal degradation curves of BC are composed of three regions. The slight weight loss in the first region is due to the loss of the absorbed water with the increase in temperature. A second weight loss, between 260 °C and 380 °C, is due to the loss of small molecular weight fractions such as hydroxyl groups of celluloses. Third weight loss occurring between 380 °C and 480 °C is due to degradation of polymeric chains and pyran structures.

Comparing the TGA curves of BC (dark curve) and BC with EMIM BF$_4$ samples, it can be easily noted that the presence of EMIM BF$_4$ promotes the cellulose degradation. A parameter that can be used to evaluate this is the maximum decomposition temperature (DTGmax) that shows the sharpest weight loss slope during decomposition. Then, looking to the maximum weight loss rate of the second decomposition region
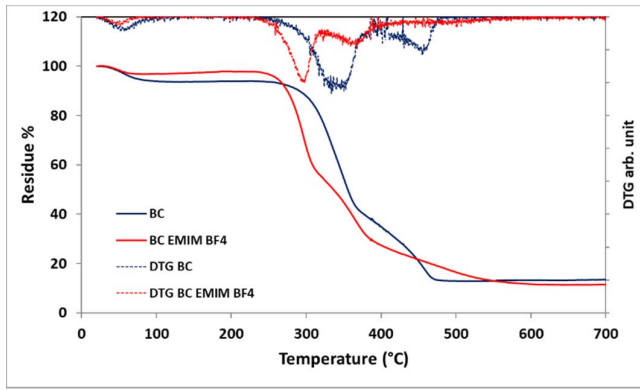
Fig. 3. TGA and DTG curves of BC and BC EMIM BF4 samples.

(dotted curves in the upper side of the Fig. 3), we can conclude that while the temperature associated with the maximum weight loss rate for BC was in the range 330 °C–355 °C, the one for BC EMIM BF$_4$ sample showed a peak of weight loss rate at 298 °C.

B. LSPR-BC Sensor System

The LSPR-BC sensor is simply obtained by sputtering gold on the slab waveguide of the previously described BC, with dimensions of 1 cm × 2 cm. The BC used in this study was provided by BioFaber s.r.l. and produced by bacteria. More details on these BC layers have already been presented in [21]. In this study (thin BC waveguides), the thickness of both configurations reported in Fig. 4(a), with and without ILs, is equal to about 36 μm, instead of 140 μm [8].

A sputtering machine (BalTec SCD 500) has been used to deposit about 60 nm in three steps (20 nm per step), each with a working current of 60 mA for a sputter time of 35 s. The multiple steps in the sputtering process were necessary to realize the deposition at low temperature. In fact, for long deposition times, the temperature in the sputter coater chamber could increase, and so the BC platform could change its characteristics. This gold layer covers the cellulose wires and sets up a kind of nanowires grid able to excite LSPR. The same sputtering process has been used in this study and in [8], [21] for all the tested BC sensor configurations.

Fig. 4(b) and (c) show, respectively, an outline and a captured picture of the experimental setup used to characterize the LSPR sensors based on thin BC slab waveguides (with and without ions inside) [8], [21]. It consists of a white light source (HL–2000–LL, manufactured by Ocean Optics, Dunedin, FL, USA), an optical coupler (50:50) in plastic optical fibers (POFs), two BC slab waveguides (1 cm × 2 cm × 36 μm), one covered with gold (i.e., the LSPR sensor) and one without gold (reference sensor), and two POFs connected with two identical spectrometers (FLAME-S-VIS-NIR-ES, manufactured by Ocean Optics, Dunedin, FL, USA) directly connected to a laptop to perform the measurements. Extrinsic optical fiber sensors exploit the fiber as a pure waveguide (patch), so the POFs have been proven to be particularly advantageous for this role due to their large diameter, great numerical aperture, easy manipulation, simple modification, excellent flexibility,

and the fact that plastic is able to withstand smaller bend radii than glass.

In the setup reported in Fig. 4, the light source exhibits a spectral emission range between 360 and 1700 nm while the spectrometers detection range is between 350 and 1000 nm.

In order to test the LSPR sensors based on thin BC slab waveguides (with and without ILs inside) various water–glycerin solutions have been used. In particular, these solutions present a refractive index ranging from 1.332 to 1.364 and have been previously characterized by an Abbe refractometer (Model RMI, Exacta + Optech GmbH, Munich, Germany).

III. Experimental Results and Discussion

A. LSPR Sensor Based on Thin BC Slab Waveguide: Configuration With Ions Inside

In [21], some of the authors have already tested an LSPR sensor based on thin BC paper (thickness of about 36 μm) with ions inside. Fig. 5 shows the LSPR spectra normalized with respect to the transmitted spectra obtained by the reference slab waveguide (i.e., the same slab waveguide with ions inside and without gold) in contact with the same surrounding medium. As clearly shown, a change in the values of the resonance wavelength and in the normalized intensity values can be observed when the refractive index of the solution upon the sensor changes. In fact, when it increases the normalized intensity value increases too while the resonance wavelength shifts toward lower values (decreases) (see inset in Fig. 5).

With regard to this configuration, Fig. 6 shows both normalized intensity at resonance wavelength (I) [see Fig. 6(a)] and the absolute value of the LSPR resonance wavelength variation ($|\Delta\lambda|$), with respect to the water ($n = 1.332$) [see Fig. 6(b)], as a function of the refractive index. In the same figure, are also reported the error bars and the linear fitting to the data for both measured values. It is important to underline that the linear fitting is a way to extrapolate a trend and allows an easy comparison between the sensors.

B. LSPR Sensor Based on Thin BC Slab Waveguide: Configuration Without Ions Inside

We have used the same approach described in subparagraph A to perform experimental measurements, relative to an LSPR sensor based on BC with the same thickness and without ions inside. In this case, we have considered a reference sensor based on BC without ILs and without gold. Fig. 7 presents the normalized LSPR spectra relative to this configuration. Also, in this case, when the refractive index of the water–glycerin solution increases, a blue shift in the resonance wavelength and an increase in the normalized intensity value are observed.

In a similar way, also for the configuration without ILs, Fig. 8(a) shows the normalized intensity at the resonance wavelength versus the refractive index, whereas Fig. 8(b) presents the absolute value of the resonance wavelength variations, with respect to water, as a function of the refractive index. In both Fig. 8(a) and (b) cases, the linear fitting is reported to extrapolate a trend and allows an easy comparison between the sensors.
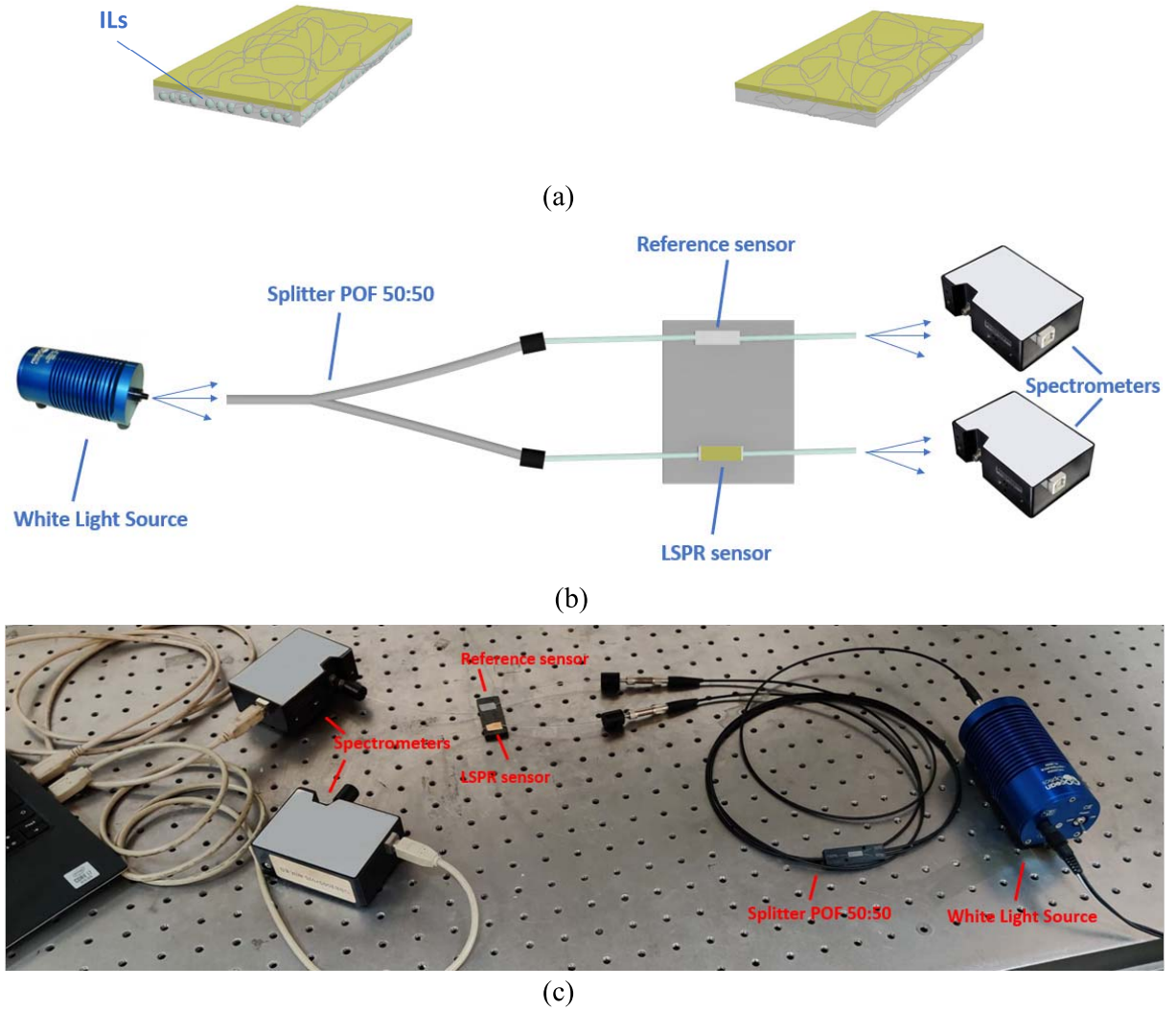
Fig. 4. (a) Outline of LSPR-BC sensors with and without ILs. (b) Scheme of the experimental setup. (c) Experimental setup.
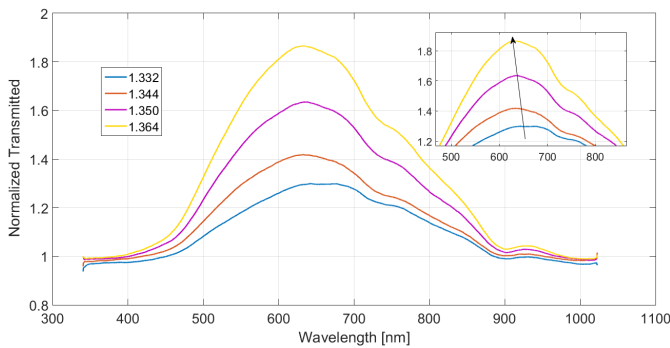

Fig. 5. Normalized Intensity LSPR spectra relative to configuration with ILs inside at different water–glycerin solutions. Inset: zoom of the resonance wavelength area.

C. Discussion

In view of comparing the performances of the two configurations described in Section III, parameters like sensitivity (S) and resolution (Δn) can be used. In particular, it is possible to term these parameters as a function of the measured value (M), i.e., the resonance wavelength or the normalized intensity, and of the refractive index (n) of the sensing layer [8].

In this case, when the refractive index of the sensing layer "n" is altered by "δn," the measured value "M" changes by "δM." So the sensitivity and the resolution of the LSPR-BC sensor can be defined as

$$S = \frac{\delta M}{\delta n} \tag{1}$$

$$\Delta n = \frac{\delta n}{\delta M} \delta M_{\text{meas}} = \frac{1}{S} \delta M_{\text{meas}} \tag{2}$$

where "δM_{meas}" is the spectral resolution of the spectrometer when the resonance wavelength is used as measured value, and the max experimentally measured variation of the normalized intensity at the resonance wavelength in the other case. In the former case, taking into account the data sheet of the spectrometer, this value is equal to 1.5 nm (spectral resolution of the spectrometer); whereas from the experimental measurements, it is equal to about 0.005 (dimensionless number) in the second case (max experimentally measured variation of the normalized intensity at the resonance) for both configurations, with and without ions inside the slab waveguide.

For the sake of clarity, we also present in Fig. 9 the variations in normalized intensity (ΔI) and resonance wavelength
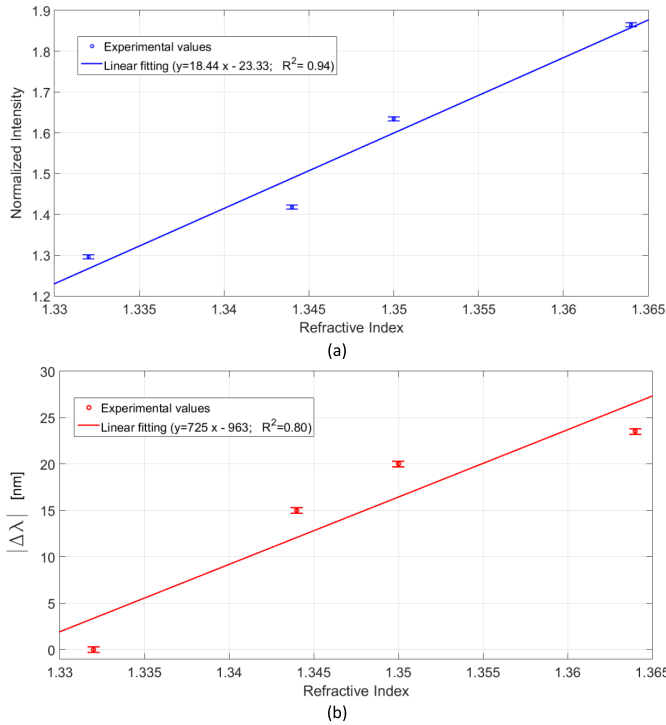
Fig. 6. Thin LSPR-BC sensors with ions. (a) Normalized intensity at resonance wavelength versus refractive index. (b) Resonance wavelength variations with respect to water ($n = 1.332$) versus refractive index.
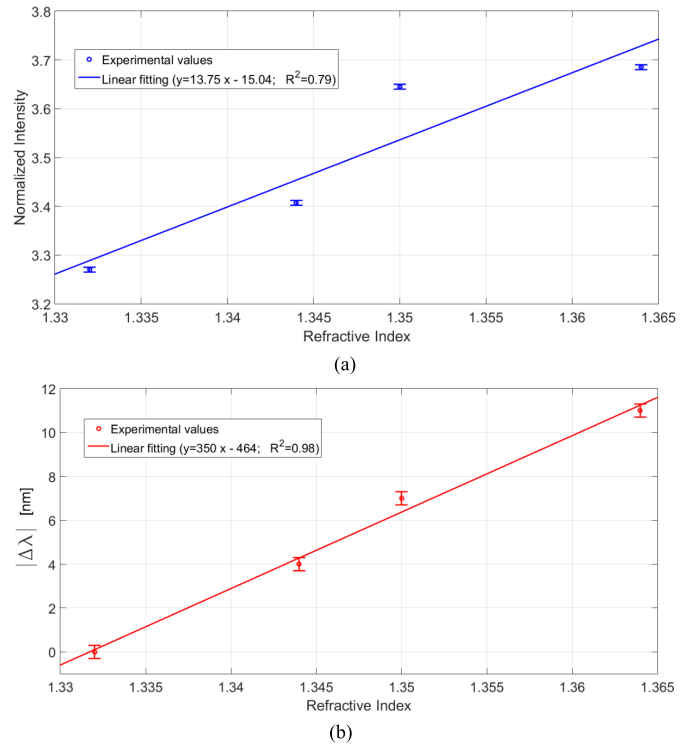

Fig. 8. Thin LSPR-BC sensors without ions. (a) Normalized intensity at resonance wavelength versus refractive index. (b) Resonance wavelength variations with respect to water ($n = 1.332$) versus refractive index.
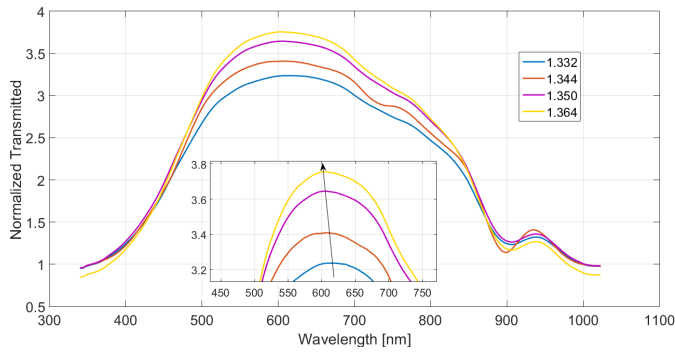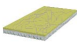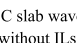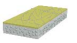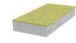

Fig. 7. Normalized Intensity LSPR spectra relative to configuration without ILs inside at different water–glycerin solutions. Inset: zoom of the resonance wavelength area.

TABLE I
COMPARATIVE ANALYSIS OF SEVERAL LSPR-BC SENSORS

Sensor Configuration	Measured Value				
	Normalized Intensity (I) [a.u.]		Resonance Wavelength (λ) [nm]		
	S_I [a.u./RIU]	Δn_I [RIU]	S_λ [nm/RIU]	Δn_λ [RIU]	Resonance type
Thin BC slab waveguide with ILs	18.44	2.7×10^{-4}	725	2×10^{-3}	blue-shift
Thin BC slab waveguide without ILs	13.75	3.6×10^{-4}	350	4.3×10^{-3}	blue-shift
Thick BC slab waveguide with ILs [8]	2.23	1.79×10^{-3}	980	1.5×10^{-3}	red-shift
Thick BC slab waveguide without ILs [8]	13.54	7.4×10^{-5}	1600	9.4×10^{-4}	red-shift

($|\Delta\lambda|$), both calculated with respect to the value measured with water as the external medium (1.332), for configurations with and without ions. It is important to underline that a simple analysis of the performances of these LSPR-BC sensor configurations has been carried out by the linear fitting.

The reported linear fitting does not imply an actual linear relationship but it has just been used to compare the performances; in fact, the Pearson's correlation coefficients of these linear fittings are lower than the standard one (see Fig. 9). Consequently, the calculation of the single values of abovementioned parameters has been carried out by employing a first-order approach. So it is important to underline that the linear fitting is only used to extrapolate a trend and allow an easy comparison between the sensors.

From (1), the sensitivity can be estimated as the slope of the linear functions presented in Fig. 9, for both the sensor configurations and both the measured values (I or λ).
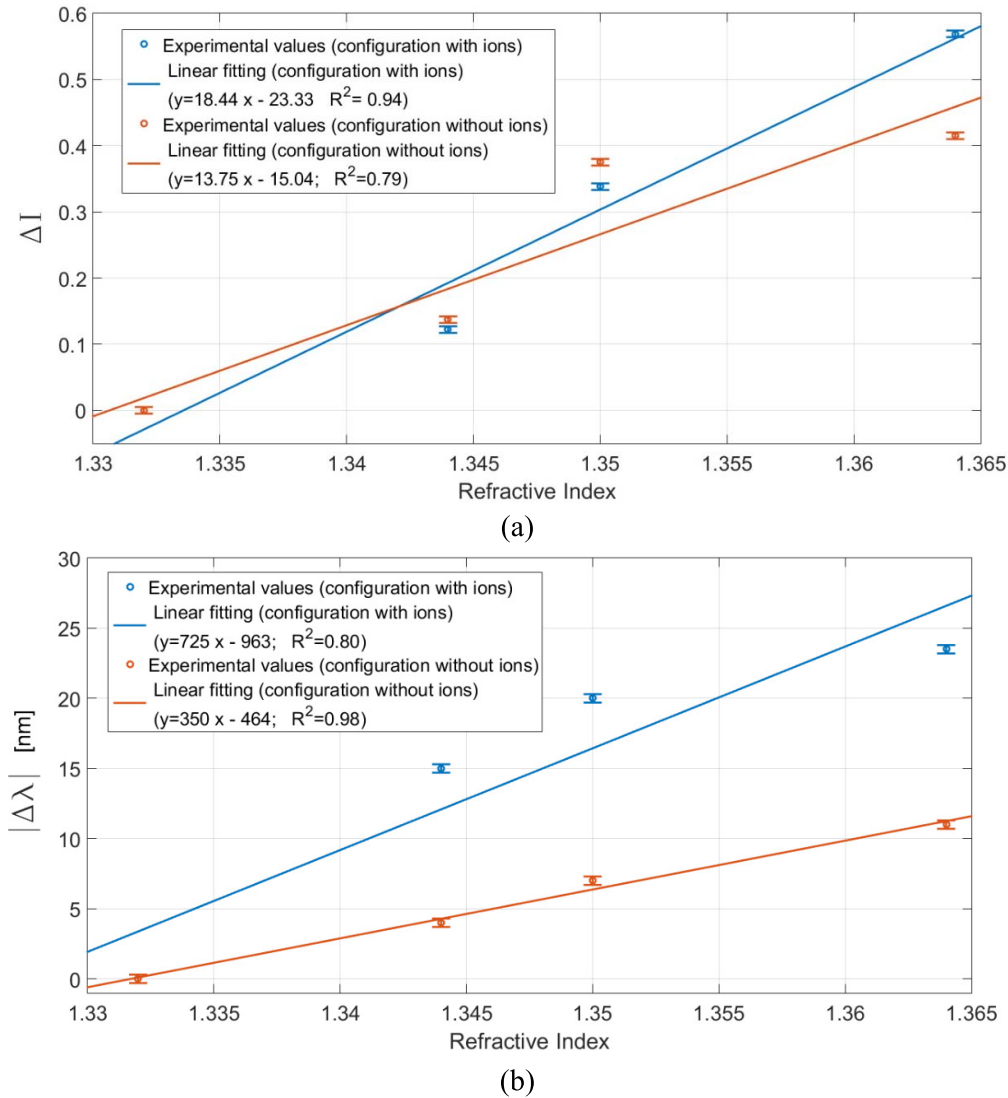
Fig. 9. Thin BC waveguides, with and without ions, configurations. (a) Normalized intensity variations (ΔI) versus refractive index. (b) Absolute value of resonance wavelength shift ($|\Delta\lambda|$) versus refractive index.

As it is clear from Fig. 9, the LSPR sensor based on a thin (about 36 μm) BC paper with ions inside shows a better sensitivity either when we consider as measured value the normalized intensity or the resonance wavelength. This result testifies that the thickness of the BC waveguide plays a key role when considering the performances. In fact, we have already conducted a similar analysis on LSPR sensors based on the same BC paper (with and without ions) but with a greater thickness (about 0.14 mm) [8]. In the latter case, the presence of the ions inside the slab waveguide makes the performances worse because the optical losses increase due to backscattering [8]. On the contrary, we have shown that, when decreasing the thickness, the presence of the ions leads to an opposite behavior by increasing the sensor performances. Another important aspect to take into account is the type of LSPR phenomenon when we consider the resonance wavelength variation. In fact, when we look at thick-slab waveguides, the resonance wavelength value increases when the refractive index of the solution placed on the sensor increases (red shift),

whereas in thin slab, the resonance wavelength value decreases if the refractive index increases (blue shift). An overview of the experimentally obtained performance parameters of the proposed LSPR-BC sensor technology is summarized in Table I.

As reported in Table II, in comparison with the other LSPR sensors, the green sensors proposed in this study offer different advantages including higher sensitivity, simpler fabrication steps, sustainability, and high reproducibility.

Concerning the tested sensors, we have performed the repeatability test by completely removing the sensor chip and then by repositioning it for five times. This procedure has been repeated for each point (refractive index) of the addressed working range.

From the results reported in Table II, considering the capability of these plasmonic probes, these disposable biodegradable extrinsic optical fiber sensors could be used combined with several types of biochemical receptors and with microfluidic cells, to realize interesting biosensors and chemical

TABLE II
COMPARATIVE ANALYSIS OF BULK SENSITIVITY OF
SEVERAL LSPR SENSORS

LSPR sensor technology	Measured Value	Bulk Sensitivity	Reference
Edge Gold-Coated Silver Nanoprisms	Resonance Wavelength	425 [nm/RIU]	E. Martinsson et al. [22]
U-Bent Plastic Optical Fiber Probes	Intensity	15.5 [a.u./RIU]	C. Christopher et al. [23]
No-core fiber with gold nanoparticles on sidewall	Resonance Wavelength	170 [nm/RIU]	Y. R. Wang et al. [24]
Periodic Gold nanorings array	Resonance Wavelength	544 [nm/RIU]	S. Wang et al. [25]
Gold Nanoparticle on Polyelectrolyte Multilayer	Intensity	13.1 [a.u./RIU]	Y. Shao et al. [26]
Triangular Ag nanoplates immobilized on glass substrate	Resonance Wavelength	204 [nm/RIU]	H. R. Hegde et al. [27]
Thin BC slab waveguide with ILs	Intensity	18.44 [a.u./RIU]	This study
Thick BC slab waveguide without ILs	Resonance Wavelength	1600 [nm/RIU]	N. Cennamo et al. [8]

sensors, useful in different application fields, as recently reported by Zhao *et al.* [28], [29].

IV. CONCLUSION

We have demonstrated that the introduction of ILs inside thin BC waveguides can improve the LSPR phenomenon while the opposite occurs in thick BC waveguides [8]. Moreover, the type of LSPR phenomenon, blue shift or red shift, changes when thin or thick BC waveguides are used, respectively. Finally, when an intensity-based LSPR sensing approach is used to realize highly sensitive sensors, as demonstrated in this work, the best configuration is based on thin BC slab waveguides with ILs inside.

ACKNOWLEDGMENT

REFERENCES

[1] R. Mangayil *et al.*, "Engineering and characterization of bacterial nanocellulose films as low cost and flexible sensor material," *ACS Appl. Mater. Interfaces*, vol. 9, no. 22, pp. 19048–19056, Jun. 2017.

[2] J.-H. Jeon, I.-K. Oh, C.-D. Kee, and S.-J. Kim, "Bacterial cellulose actuator with electrically driven bending deformation in hydrated condition," *Sens. Actuators B, Chem.*, vol. 146, no. 1, pp. 307–313, Apr. 2010.

[3] F. Esa, S. M. Tasirin, and N. A. Rahman, "Overview of bacterial cellulose production and application," *Agricult. Agricult. Sci. Procedia*, vol. 2, pp. 113–119, Nov. 2014.

[4] S.-S. Kim, J.-H. Jeon, C.-D. Kee, and I.-K. Oh, "Electro-active hybrid actuators based on freeze-dried bacterial cellulose and PEDOT:PSS," *Smart Mater. Struct.*, vol. 22, no. 8, Aug. 2013, Art. no. 085026.

[5] G. Di Pasquale, S. Graziani, A. Pollicino, and C. Trigona, "Performance characterization of a biodegradable deformation sensor based on bacterial cellulose," *IEEE Trans. Instrum. Meas.*, vol. 69, no. 5, pp. 2561–2569, May 2020.

[6] G. D. Pasquale, S. Graziani, A. Pollicino, and C. Trigona, "A bacterial cellulose based mass sensor," in *Proc. IEEE Int. Symp. Meas. Netw. (M&N)*, Catania, Italy, Jul. 2019, pp. 1–4.

[7] G. Di Pasquale, S. Graziani, A. Pollicino, and C. Trigona, "Green inertial sensors based on bacterial cellulose," in *Proc. IEEE Sensors Appl. Symp. (SAS)*, Sophia Antipolis, France, Mar. 2019, pp. 1–4.

[8] N. Cennamo *et al.*, "An eco-friendly disposable plasmonic sensor based on bacterial cellulose and gold," *Sensors*, vol. 19, no. 22, p. 4894, Nov. 2019.

[9] X. D. Wang and O. S. Wolfbeis, "Fiber-optic chemical sensors and biosensors (2013–2015)," *Anal. Chem.*, vol. 88, no. 1, pp. 203–227, 2016.

[10] A. K. Sharma, R. Jha, and B. D. Gupta, "Fiber-optic sensors based on surface plasmon resonance: A comprehensive review," *IEEE Sensors J.*, vol. 7, no. 8, pp. 1118–1129, Aug. 2007.

[11] A. K. Sharma, A. K. Pandey, and B. Kaur, "A review of advancements (2007–2017) in plasmonics-based optical fiber sensors," *Opt. Fiber Technol.*, vol. 43, pp. 20–34, Jul. 2018.

[12] A. Leung, P. M. Shankar, and R. Mutharasan, "A review of fiber-optic biosensors," *Sens. Actuators B, Chem.*, vol. 125, no. 2, pp. 688–703, 2007.

[13] S. K. Srivastava, R. K. Verma, and B. D. Gupta, "Theoretical modeling of a localized surface plasmon resonance based intensity modulated fiber optic refractive index sensor," *Appl. Opt.*, vol. 48, no. 19, pp. 3796–3802, 2009.

[14] M. Rani, N. K. Sharma, and V. Sajal, "Localized surface plasmon resonance based fiber optic sensor with nanoparticles," *Opt. Commun.*, vol. 292, pp. 92–100, Apr. 2013.

[15] Q. Wang, J.-Y. Jing, X.-Z. Wang, L.-Y. Niu, and W.-M. Zhao, "A D-shaped fiber long-range surface plasmon resonance sensor with high Q-factor and temperature self-compensation," *IEEE Trans. Instrum. Meas.*, vol. 69, no. 5, pp. 2218–2224, May 2020.

[16] A. A. D. Melo, T. B. D. Silva, M. F. D. S. Santiago, C. D. S. Moreira, and R. M. S. Cruz, "Theoretical analysis of sensitivity enhancement by graphene usage in optical fiber surface plasmon resonance sensors," *IEEE Trans. Instrum. Meas.*, vol. 68, no. 5, pp. 1554–1560, May 2019.

[17] S. Rampazzi, G. Danese, F. Leporati, and F. Marabelli, "A localized surface plasmon resonance-based portable instrument for quick on-site biomolecular detection," *IEEE Trans. Instrum. Meas.*, vol. 65, no. 2, pp. 317–327, Feb. 2016.

[18] N. Cennamo, D. Massarotti, L. Conte, and L. Zeni, "Low cost sensors based on SPR in a plastic optical fiber for biosensor implementation," *Sensors*, vol. 11, no. 12, pp. 11752–11760, Dec. 2011.

[19] N. Cennamo, L. Zeni, F. Arcadio, E. Catalano, and A. Minardo, "A novel approach to realizing low-cost plasmonic optical fiber sensors: Light-diffusing fibers covered by thin metal films," *Fibers*, vol. 7, no. 4, p. 34, Apr. 2019.

[20] N. Cennamo, F. Mattiello, and L. Zeni, "Slab waveguide and optical fibers for novel plasmonic sensor configurations," *Sensors*, vol. 17, no. 7, p. 1488, Jun. 2017.

[21] N. Cennamo *et al.*, "An LSPR sensor based on a thin slab waveguide of bacterial cellulose," in *Proc. IEEE Int. Instrum. Meas. Technol. Conf. (IMTC)*, Dubrovnik, Croatia, May 2020, pp. 1–5.

[22] E. Martinsson *et al.*, "Local refractive index sensing based on edge gold-coated silver nanoprisms," *J. Phys. Chem. C*, vol. 117, no. 44, pp. 23148–23154, Nov. 2013.

[23] C. Christopher, A. Subrahmanyam, and V. V. R. Sai, "Gold sputtered U-bent plastic optical fiber probes as SPR- and LSPR-based compact plasmonic sensors," *Plasmonics*, vol. 13, no. 2, pp. 493–502, Apr. 2018.

[24] Y. R. Wang, Z. Q. Tou, C. L. Zhao, P. L. So, and C. C. Chan, "Localized surface plasmon resonance refractometer based on no-core fiber," in *Proc. 25th Int. Conf. Opt. Fiber Sensors*, Jeju, South Korea, Apr. 2017, pp. 1–4.

[25] S. Wang *et al.*, "The investigation of an LSPR refractive index sensor based on periodic gold nanorings array," *J. Phys. D, Appl. Phys.*, vol. 51, no. 4, Jan. 2018, Art. no. 045101.

[26] Y. Shao, S. Xu, X. Zheng, Y. Wang, and W. Xu, "Optical fiber LSPR biosensor prepared by gold nanoparticle assembly on polyelectrolyte multilayer," *Sensors*, vol. 10, no. 4, pp. 3585–3596, Apr. 2010.

[27] H. R. Hegde, S. Chidangil, and R. K. Sinha, "Refractive index sensitivity of triangular Ag nanoplates in solution and on glass substrate," *Sens. Actuators A, Phys.*, vol. 305, Apr. 2020, Art. no. 111948.

[28] Y. Zhao, X.-G. Hu, S. Hu, and Y. Peng, "Applications of fiber-optic biochemical sensor in microfluidic chips: A review," *Biosensors Bioelectron.*, vol. 166, Oct. 2020, Art. no. 112447.

[29] Y. Zhao, R.-J. Tong, F. Xia, and Y. Peng, "Current status of optical fiber biosensor based on surface plasmon resonance," *Biosensors Bioelectron.*, vol. 142, Oct. 2019, Art. no. 111505.

Nunzio Cennamo was born in Italy in 1975. He received the master's degree in electronic engineering and the Ph.D. degree in electronic engineering from the Second University of Naples, Naples, Italy.

He is currently a Professor of electronics at the University of Campania Luigi Vanvitelli, Naples. He is a cofounder of the spin off "MORESENSE srl," Milan, Italy (Fondazione Filarete, Milan). He has authored more than 100 international journal and conference papers and seven patents. His research interests include the design and fabrication of optical fiber sensors, chemical sensors, biosensors, and optoelectronic devices.

Dr. Cennamo is currently an Associate Editor of the *Photonics Research* (OSA) and the *Applied Sciences* (MDPI), a member of the Editorial Board and several times Guest Editor of Sensors (MDPI). He is an Organizer and a General Chair of the 7th International Symposium on Sensor Science (I3S 2019), May 9, 2019–May 11, 2019, Naples, Italy. He is an invited speaker in webinars and international conferences.

Carlo Trigona (Member, IEEE) received the M.S. degree (*cum Laude*) in automation engineering and control of complex systems and the Ph.D. degree in electronic, automation, and control of complex systems from the University of Catania, Catania, Italy, in 2006 and 2009, respectively.

He worked as a post-doc and a Lecturer at University Montpellier II–LIRMM, Montpellier, France, from 2010 to 2011, and at DIEEI, University of Catania, from 2011 to 2017, and as a post-doc at the Chemnitz University of Technology, Chemnitz, Germany, from 2017 to 2018. From 2018 to 2020, he worked as an Assistant Professor of electronic instrumentation and measurements at DIEEI, University of Catania. Since 2020, he has been a tenure track Professor of electronic instrumentation and measurements at DIEEI, University of Catania. Regarding his research activity, his first paper appeared in 1997; and, at the moment, he has coauthored more than 200 scientific publications, with more than 1400 total citations, which include chapters in books, articles in international journals, and proceedings of international conferences and patents. His research interests include sensors, transducers, MEMS, NEMS, fluxgate magnetometers, energy harvesting, and green and biodegradable sensors.

Dr. Trigona contributes in the Instrumentation and Measurement community with several activities also including editor and reviewer for several prestigious journals starting from 2006, until now. He received several awards for his research activity since 2007, including the 2020 IEEE I&M Outstanding Young Engineer Award for his outstanding contribution to the advancement of I&M concept in sensors and transducers for energy harvesting.

Salvatore Graziani (Member, IEEE) received the M.S. degree in electronic engineering and the Ph.D. degree in electrical engineering from the Università degli Studi di Catania, Catania, Italy, in 1990 and 1994, respectively.

Since 1990, he has been with the Dipartimento di Ingegneria Elettrica, Elettronica e Informatica, Università di Catania, where he is currently an Associate Professor of electric and electronic measurement and instrumentation. He has coauthored several scientific articles and books. His primary research interests lie in the field of sensors and actuators, and soft sensors.

Luigi Zeni received the master's degree (*summa cum laude*) in electronic engineering from the University of Naples, Naples, Italy, in 1988, and the Ph.D. degree in electronics and computer science from the Italian Ministry of University, Rome, Italy, in 1992.

He worked at TU-DELFT (NL), Delft, The Netherlands, as a Visiting Scientist. He has been a national coordinator of PRIN projects, and a scientific coordinator of research contracts with public and private institutions and responsible for projects funded within the 7th FP of the EU. He is currently a Full Professor of electronics at the University of Campania L. Vanvitelli, Caserta, Italy, and a President of the Research Consortium on Advanced Remote Sensing Systems–CO.RI.S.T.A. (www.corista.eu). From 2001 to 2012, he was a Vice Director of the Department of Information Engineering. He is also a founder of the spin-off company OPTOSENSING dealing with structural and environmental monitoring by optical fiber sensors. He has authored more than 140 articles in international journals and 150 publications at international conferences and holds 12 patents. His main research interests include optical fiber sensors for distributed measurements of deformation and temperature, optoelectronic integrated sensors, and biosensors.

Dr. Zeni has been a member of the Management Committee of the COST 299 "Optical fibers for new challenges facing the information society" and of the COST TD1001è "Novel and Reliable Optical Fiber Sensor Systems for Future Security and Safety Applications."

Francesco Arcadio was born in Italy in 1991. He received the master's degree in electronic engineering in 2018, from University of Campania "Luigi Vanvitelli," Caserta, Italy, where he is currently pursuing the Ph.D. degree.

His research interests include the design and fabrication of optical sensors and biosensors.

Liu Xiaoyan received the M.S. and Ph.D. degrees from the School of astronautics, Harbin Institute of Technology, Harbin, China, in 2008 and 2014, respectively.

She is currently a Lecturer from the College of Electrical and Electronic Engineering, Changchun University of Technology, Changchun, China.

Giovanna Di Pasquale received the M.S. degree (*summa cum laude*) in chemistry from the University of Catania, Catania, Italy, in 1981.

She is currently an Associate Professor of chemical fundamentals of technology from the Chemical Science Department, University of Catania. She has authored more than 60 publications on international refereed journals and a considerable amount of communications to national and international conferences. Her research interests include synthesis and characterization of polymeric smart materials.

Antonino Pollicino received the M.S. degree in chemistry from the University of Catania, Catania, Italy, in 1983.

He has a position of Full Professor of science and technology of materials with the University of Catania. His scientific activity is mainly focused on polymeric materials. He has authored more than 100 publications on international refereed journals and a considerable amount of communications to national and international conferences. He spent several research periods abroad (U.K. and Australia) working on advanced polymeric materials.